

# Noncritical phase-matched lithium triborate optical parametric oscillator for high resolution coherent anti-Stokes Raman scattering spectroscopy and microscopy

M. Jurna,<sup>a)</sup> J. P. Korterik, and H. L. Offerhaus

Optical Techniques Group<sup>b)</sup>, Department of Science and Technology, MESA<sup>+</sup> Institute for Nanotechnology, University of Twente, Enschede, Overijssel 7500 AE, The Netherlands

C. Otto

BioPhysical Engineering Group,<sup>c)</sup> Department of Science and Technology, MESA<sup>+</sup> Institute for Nanotechnology, University of Twente, Enschede, Overijssel 7500 AE, The Netherlands

(Received 10 October 2006; accepted 14 November 2006; published online 21 December 2006)

An efficient, widely tunable, narrow-bandwidth, green-pumped, noncritical phase-matched lithium triborate based optical parametric oscillator (OPO) is applied to coherent anti-Stokes Raman scattering (CARS) spectroscopy and microscopy. The tunable signal beam (740–930 nm) of the OPO is combined with the fundamental of a Nd:YVO<sub>4</sub> pump laser (1064 nm, 15 ps) to obtain high resolution vibrational spectra of molecules around the CH vibrational stretch (2700–3100 cm<sup>-1</sup>). The straightforward and convenient tunability of the OPO is demonstrated by CARS microscopy for the identification of different polymer microparticles on the same substrate. © 2006 American Institute of Physics. [DOI: 10.1063/1.2420773]

Imaging and visualization of biological processes in complex environments, such as living cells, is a subject of wide interest.<sup>1–3</sup> High spatial resolution and chemical selectivity are the main parameters of interest. The combination of vibrational spectroscopy and nonlinear microscopy provides a direct and noninvasive technique to localize and identify structures of different chemical compositions.<sup>4</sup> Coherent anti-Stokes Raman scattering (CARS) is a well known technique for vibrational spectroscopy.<sup>5–7</sup> CARS is a four-photon process, where a pump photon of frequency  $\omega_p$ , a Stokes photon of frequency  $\omega_s$ , and probe photon of frequency  $\omega'_p$  (often taken the same as the pump frequency<sup>8</sup>) interact with the sample and generate an anti-Stokes photon of frequency  $\omega_{as} = \omega_p - \omega_s + \omega'_p$ . The CARS signal is resonantly enhanced when the difference frequency  $\omega_p - \omega_s$  coincides with a molecular vibrational level transition. By tuning the difference frequency, the unique vibrational spectrum of a molecule can be obtained and used for imaging. The advantage of CARS over spontaneous Raman scattering is the one-photon fluorescence-free monochromatic signal that can be detected with a high collection efficiency. Furthermore, the CARS signal intensity depends quadratically on the pump field intensity and linearly on the Stokes field intensity so that pulsed excitation can result in signal rates much higher than in spontaneous Raman scattering. In a highly collimated CARS setup the inherent presence of a nonresonant background signal is not a limiting factor.<sup>9,10</sup>

Green-pumped optical parametric oscillators (OPOs) have been demonstrated previously<sup>11,12</sup> and a picosecond synchronously green-pumped OPO (Ref. 13) is an ideal source for the tunable wavelength for CARS spectroscopy and microscopy: it provides wavelengths in the optimal region (near infrared), synchronized pulses, and reasonable bandwidth.<sup>14</sup> The nonlinear crystal in this OPO is a

Brewster-angled lithium triborate (LBO) LiB<sub>3</sub>O<sub>5</sub>. This crystal has a high damage threshold, low linear absorption, low cost, and due to the zero beam walk-off, LBO crystals can be made long to compensate the moderate nonlinear coefficient of 0.8 pm/V. The noncritical phase-matching means that all parts remain fixed during scanning (no rotating parts). Since the beam pointing is defined by the flat output coupler, it is independent of the signal wavelength and no adjustments are required in the CARS setup. Only the OPO cavity length has to be adjusted for the variation in round-trip time.

A layout of the setup of the OPO can be seen in Fig. 1. The pump source is a mode locked Nd:YVO<sub>4</sub> based laser (Vanguard 2000-HM532, Spectra-Physics) at 1064 nm, which is doubled to 532 nm. It generates approximately 5 W at 1064 nm with pulses of 15 ps at a repetition rate of 80 MHz and this light is partially doubled to 2 W of 12 ps pulses at 532 nm. The beam is expanded to a waist radius of 3.4 mm at the focusing lens. The OPO cavity is singly resonant for the signal wave and is formed by two concave mirrors, two flat mirrors, and a 6% plane output coupler. The two extra plane mirrors were introduced to reduce the resonator size to fit a breadboard of 90 × 30 cm<sup>2</sup>. The mirrors are

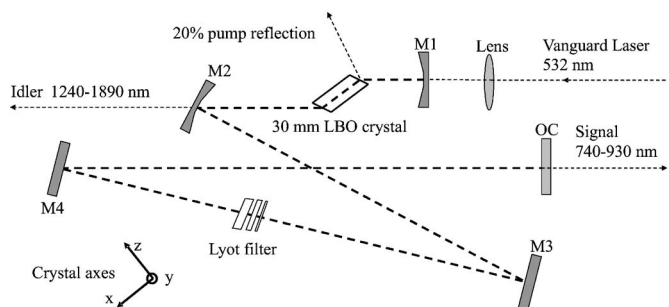


FIG. 1. Schematic of the OPO. The resonator consists of a 30 mm long Brewster-angled LBO crystal inside a temperature controlled oven, two concave mirrors, M1 (100 mm ROC) and M2 (250 mm ROC), two plane mirrors M3 and M4, and a 6% output coupler (OC). A 200 mm lens focuses the 532 nm pump beam in the LBO crystal.

<sup>a)</sup>Electronic mail: m.jurna@utwente.nl

<sup>b)</sup>URL: <http://ot.tnw.utwente.nl/>

<sup>c)</sup>URL: <http://bpe.tnw.utwente.nl/>

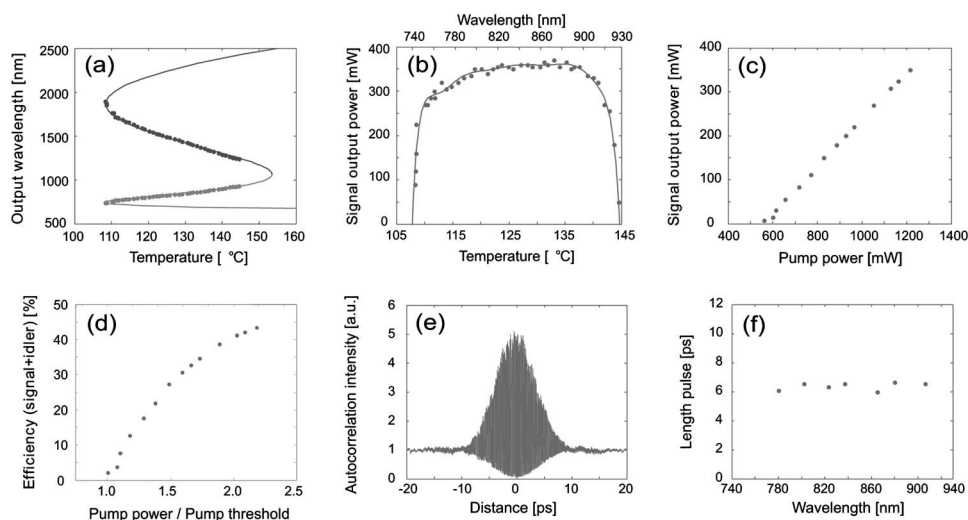


FIG. 2. (a) Temperature tuning curve of the noncritical phase-matched LBO, (b) OPO output power vs temperature (bottom) and wavelength (top), (c) OPO pump depletion, (d) OPO output, (e) autocorrelation of signal OPO pulse at 780 nm, and (f) length of OPO pulses for different signal wavelengths.

highly reflective ( $R > 99.9\%$ ) over the range of 740–930 nm and the transmission at 532 nm is higher than 98%. The output coupler was placed on a precision translation stage with a motor-controlled micrometer. The LBO crystal is 30 mm long and Brewster angled ( $59^\circ$ ) for the signal. The crystal is cut for a type I ( $e \rightarrow o + o$ ) noncritical phase-matching in the  $xy$  plane ( $\theta = 90^\circ$  and  $\phi = 0^\circ$ ). The three beams propagate along the  $x$  direction, where the pump beam is polarized along the  $y$  axis and the signal and idler beam are polarized along the  $z$  axis. The temperature of the crystal can be varied between ambient and 200 °C with a stability of 0.1 °C. The concave mirrors have a radius of curvature (ROC) of 100 (M1) and 250 mm (M2), respectively. The angle of incidence on the second concave mirror (M2) is  $18^\circ$  to compensate for astigmatism introduced by the Brewster-angled LBO crystal.<sup>15</sup> The signal bandwidth is reduced by a Lyot filter.

The performance of the OPO is shown in Fig. 2 for an average pump power of 1.2 W in the nonlinear crystal. At each measurement the signal power is maximized by minimization of the cavity length mismatch between pump laser and the OPO. The signal output power exceeds 300 mW over the full operation range, which is more than sufficient for CARS spectroscopy and microscopy. The OPO has a threshold of  $\sim 550$  mW of input pump power and the pulse length of the OPO signal output is  $\sim 6.4$  ps over the entire tuning range. The reduced dynamic range of the autocorrelation trace is attributed to residual misalignment.

To demonstrate the capabilities as a source for CARS spectroscopy, the tunable signal beam (740–930 nm) is combined with the fundamental of the Vanguard laser (1064 nm) for the detection of the CH vibrational stretch modes in organic molecules. These modes produce strong resonances and a large signal at low excitation power,<sup>4</sup> so that a Forward CARS setup can be used. The polarizations of the pump and Stokes beams are aligned parallel and can be controlled by a  $\lambda/2$  plate in both beams. The pump and Stokes beams are combined on a dichroic (HR: 1064 nm; HT: 700–900 nm) mirror and focused by a 0.65 NA (numerical aperture) objective lens in the sample. The sample is held in a piezoscanned ( $80 \times 80 \mu\text{m}^2$ ) sample holder for imaging. The collected and filtered CARS signal is detected on a Hamamatsu (R1463)

photomultiplier tube. The signal can be further filtered by the addition of a chopper and lock-in amplifier.

In Fig. 3(a) the CARS vibrational spectrum of toluene is shown, for a few tens of milliwatts in the pump and Stokes beams. The CARS signal is corrected for the variation in output power. Every second a measurement is taken of the pump wavelength and the CARS signal. The total vibrational scan is obtained over 800 wavenumbers in 26 min, where the scanning speed is presently limited by the thermalization of the crystal. A high spectral resolution around  $2 \text{ cm}^{-1}$  is obtained, due to the smooth and stable temperature scanning of the OPO. Comparison of the CARS vibrational spectrum of toluene with the spontaneous Raman spectrum, Fig. 3(b), shows that the vibrational frequencies can be assigned with a one-to-one correspondence. Figure 4 also shows the measured CARS vibrational spectrum of polymethylmetacrylate (PMMA).

To demonstrate the practical advantage of the tunability of this OPO for CARS microscopy we show localization and identification of structures of different chemical composition. Different polymer microparticles of similar size and shape on the same substrate are used. A mixture of PMMA and polystyrene (PS) microspheres is imaged at different pump wavelengths. In Fig. 4 the vibrational spectra are displayed and it can be seen that tuning the OPO to 804 nm only the PS microspheres are imaged. Tuning the OPO to 810 nm, the PMMA microspheres are imaged (strong signal), as well as the PS spheres (weak signal). The images can be seen in Figs. 5(a) and 5(b). These images show a lateral resolution of less than 500 nm and demonstrate the possibility of chemical

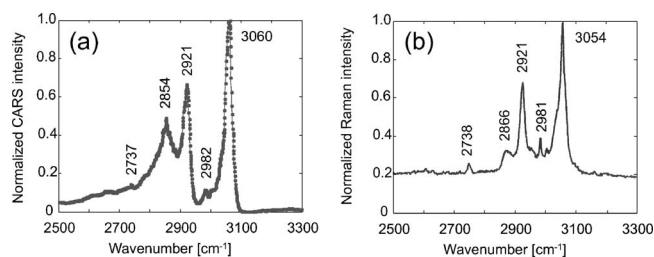


FIG. 3. (a) CARS vibrational spectrum of toluene and (b) Raman spectrum.

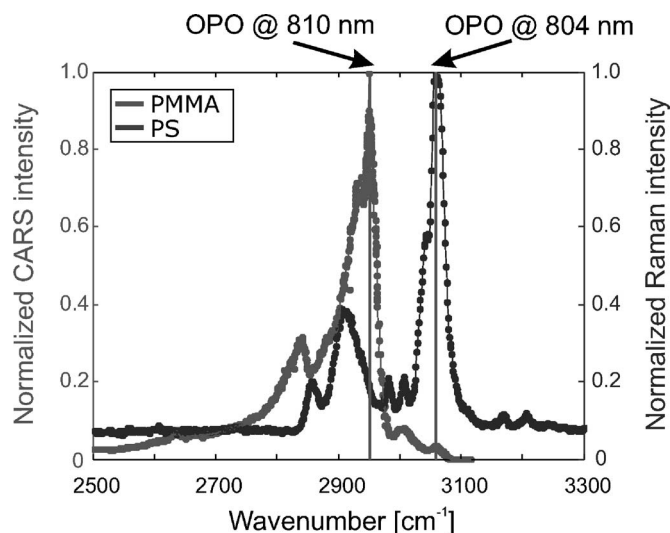


FIG. 4. CARS vibrational spectrum of PMMA and spontaneous Raman spectrum of PS Ref. 16.

specificity without labeling. The axial resolution was measured separately by an axial scan through the bead to be less than  $1\ \mu\text{m}$ . No attempt was made in these measurements to suppress the nonresonant background. When the CARS images are overlapped, spheres made of PMMA and PS can be easily distinguished. The result is shown in Figs. 5(c) and 5(d) for 4 and  $1\ \mu\text{m}$  spheres.

In conclusion, we demonstrate a highly efficient, widely tunable, narrow-bandwidth, green-pumped OPO based on a noncritical phase-matching Brewster-angled LBO crystal, temperature tunable in the range of 740–930 nm. Combining the signal wavelength of the OPO with the fundamental 1064 nm of the pump laser provides high spectral resolution ( $2\ \text{cm}^{-1}$ ). CARS vibrational microscopy is demonstrated by the localization and identification of different polymer microparticles of the same size and shape with a lateral resolution of less than 500 nm and an axial resolution of less than  $1\ \mu\text{m}$ .

This work is part of a research project of the “Stichting voor Fundamenteel Onderzoek der Materie (FOM),” which is financially supported by the “Nederlandse Organisatie voor Wetenschappelijk Onderzoek (NWO)” and by NanoNed, a nanotechnology program of the Dutch Ministry of Economic Affairs.

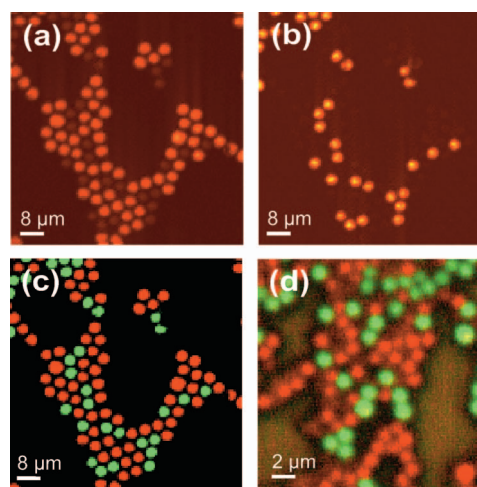


FIG. 5. (Color) [(a) and (b)] Images ( $80 \times 80\ \mu\text{m}^2$ ) of a mixture of  $4.0\ \mu\text{m}$  diameter PMMA spheres with  $4.0\ \mu\text{m}$  diameter PS spheres. (a) is obtained at 804.0 nm pump wavelength and (b) is obtained at 810 nm pump wavelength. For the Stokes 1064 nm is used. The images contain  $128 \times 128$  pixels collected at 20 ms/pixel. [(c) and (d)] Combined figures of the images scanned at 804 nm (showed in green) and 810 nm (showed in red). (c) Mixture of  $4\ \mu\text{m}$  PMMA and PS spheres. (d) Mixture of  $1\ \mu\text{m}$  PMMA and PS spheres.

- <sup>1</sup>E. Betzig, G. H. Patterson, R. Sougrat, O. W. Lindwasser, S. Olenych, J. S. Bonifacino, M. W. Davidson, J. Lippincott-Schwartz, and H. F. Hess, *Science* **313**, 1642 (2006).
- <sup>2</sup>M. Navratil, G. A. Mabbott, and E. A. Arriaga, *Anal. Chem.* **78**, 4005 (2006).
- <sup>3</sup>H. J. van Manen, Y. M. Kraan, D. Roos, and C. Otto, *Proc. Natl. Acad. Sci. U.S.A.* **102**, 10159 (2005).
- <sup>4</sup>J. X. Cheng, A. Volkmer, and X. S. Xie, *J. Opt. Soc. Am. B* **19**, 1363 (2002).
- <sup>5</sup>A. Voroshilov, C. Otto, and J. Greve, *Appl. Spectrosc.* **50**, 78 (1996).
- <sup>6</sup>G. Petrov and V. Yakovlev, *Opt. Express* **13**, 1299 (2005).
- <sup>7</sup>H. Kano and H. Hamaguchi, *Opt. Express* **14**, 2798 (2006).
- <sup>8</sup>E. O. Potma, D. J. Jones, J. X. Cheng, X. S. Xie, and J. Ye, *Opt. Lett.* **27**, 1168 (2002).
- <sup>9</sup>J. X. Cheng, L. D. Book, and X. S. Xie, *Opt. Lett.* **26**, 1341 (2001).
- <sup>10</sup>E. O. Potma, C. L. Evans, and X. S. Xie, *Opt. Lett.* **31**, 241 (2006).
- <sup>11</sup>S. Akhmanov, N. Koroteev, and A. Kolodnykh, *J. Raman Spectrosc.* **2**, 239 (1974).
- <sup>12</sup>F. Ganikhanov, S. Carrasco, X. S. Xie, M. Katz, W. Seitz, and D. Kopf, *Opt. Lett.* **31**, 1292 (2006).
- <sup>13</sup>T. Tukker, C. Otto, and J. Greve, *Opt. Commun.* **154**, 83 (1998).
- <sup>14</sup>J. X. Cheng and X. S. Xie, *J. Phys. Chem. B* **108**, 827 (2004).
- <sup>15</sup>T. Tukker, C. Otto, and J. Greve, *J. Opt. Soc. Am. B* **15**, 2455 (1998).
- <sup>16</sup>X. S. Xie and H. L. Offerhaus, measured at CARS Workshop, Xie-group, 2006 (unpublished).